11th U. S. National Combustion Meeting
Organized by the Western States Section of the Combustion Institute
March 24–27, 2019
Pasadena, California

Detailed soot modeling of mixing controlled compression ignition engines

Tyler Strickland[1], Sage L. Kokjohn[1]

[1]Engine Research Center, University of Wisconsin - Madison, Madison-WI, USA
[*]Corresponding Author Email: testrickland@wisc.edu

Abstract Most soot simulation is done using relatively simple models that only provide basic information regarding general soot mass due to the high computational cost of more complex models. In this work, a stochastic model capable of detailed soot description has been implemented in a hybrid fashion such that a relatively fast conventional combustion simulation followed by many independent highly parallelizable soot simulations can be used. The model is used to characterize the origin and advection of soot for a diesel engine with a triple injection scheme.

Keywords: Soot, Stochastic, Monte-Carlo, Lagrangian Parcel

1. Introduction

Soot simulation for engine combustion applications ranges from simple semi-empirical models [1] to more complex solutions of the population balance equations [2]. Commonly, conclusions are drawn from very simple phenomenological multistep models, which are computationally inexpensive, but only provide a single variable, mass or volume fraction, describing soot and struggle to make accurate predictions without case specific tuning. The next steps in complexity and the state-of-the-art in industry software are the method of moments [3] or sectional models [2] that have multiple variables predicting particle distributions. Both approaches are limited in their ability to describe details of the particle morphology. Additionally, the method of moments requires assumptions about the shape of the distribution [4] and the sectional model can only resolve a discretized probability density function (PDF).

Stochastic solutions to the population balance equations (e.g., Celnik et al. [5]) can retain more features of the particle ensemble, enabling a detailed description of the particle morphology at the expense of increased computational cost. The detailed description of the particle morphology may improve the ability to predict key features driving the soot formation process. Previous work by Morgan *et al.* [6] included consideration of primary particle diameter and location to describe particle morphology. Celnik *et al.* [5] added variables to describe the types of active sites on the particles for surface reaction models. Typically, stochastic soot simulations are constrained to simplified configurations (e.g., laminar premixed flames [7]) due to the complexity and computational cost of implementing a stochastic model in a nonhomogeneous, three-dimensional domain.

Previous work [8] has introduced and validated a methodology to implement stochastic soot models in 3D; however, the computational cost of the model is still relatively unbounded and usually expensive. Instruction-wise, the standard coagulation kernel size grows by the number of stochastic particles squared [9]. Simulations requiring consideration of particles that are orders of

magnitude less prevalent than other particles, like accumulation and inception mode particles, can be extremely costly. That is, simulations with information for particles that only occur 1:10,000 of the time cost 100 times more than simulations with information for particles that only occur 1:1,000 of the time. Additionally, in the 3D solution method, every time step is dependent on the slowest parcel. Memory-wise, a single stochastic ensemble can easily require over a Mb of memory and every cell capable of producing non-negligible soot must have a parcel in it. 2^{15} (32768) particles described by 8 floating point numbers each cost more than a Mb. If the Eulerian mesh has more than 1,000,000 cells with one-tenth of the cells producing non-negligible soot, the soot simulation will require more than 100 Gb.

The present work focuses on further reducing the computational cost of detailed morphological soot data provided by stochastic 3D soot model via hybridizing a conventional and stochastic soot model. The hybrid model implements a conventional soot solution during the combustion simulation and a re-calculation via stochastic means in a post processing fashion.

2. Methods

Soot is modeled using SWEEP, a stochastic modified Monte-Carlo method soot model developed by Celnik *et al.* [10], and Patterson *et al.* [9] and distributed by the Cambridge CoMo group. The model includes a majorant kernel developed Goodson *et al.* [11] to replace the coagulation kernel and linear process deferment algorithm (LDPA) developed by Patterson *et al*. [9] to increase the computational speed. SWEEP manages a random ensemble of virtual soot particles that represent the total population. As the number of representative particles increases, the law of large numbers dictates that the representation becomes more accurate [7]. In the current SWEEP implementation, the representative virtual particles are described by the constituent number of carbon and hydrogen atoms, characteristic diameter, surface area, volume, and age and are controlled by the Smoluchouski population balance equation

$$\frac{\partial n(x_i,t)}{\partial t} = \frac{1}{2}\sum_{j=1}^{i-1} K(x_i - x_j, x_j)n(x_i - x_j, t)n(x_j, t) - \sum_{j=1}^{\infty} K(x_i, x_j)n(x_i, t)n(x_j, t), \qquad (1)$$

where $n(x_i, t)$ is the number of particles of type x_i at the time t, $K(x_i, x_j)$ is the coagulation kernel for particles of type x_i and x_j.

The population balance is shifted by random events that occur at a frequency determined by physical sub-models. These events are virtual realizations of the four major soot formation phenomena: nucleation, coagulation, surface reactions, and agglomeration [12]. That is, the events change the parameters of the virtual particles. The specific events considered in this work include inception via pyrene, condensation of pyrene, oxidation via O_2 and OH, addition of acetylene, and agglomeration. Inception is modeled as a two-body collision in the gas phase between pyrene molecules using the collision transition kernel formulated by Patterson *et al*. [13] given by

$$K^{tr} = \left(\frac{1}{K^{sf}} + \frac{1}{K^{fm}}\right)^{-1}, \qquad (2)$$

where K^{sf} is the slip flow kernel, K^{fm} is the free molecular kernel, and K^{tr} is the transition kernel. Similar to other studies (e.g., [12] [14]), pyrene is used as the soot inception species. Condensation is modeled as a free-molecular collision between an existing soot particle and a PAH. Coagulation is a two body collision between two existing soot particles with the same collision model kernel used for inception and described by Patterson *et al*. [13]. O_2 and OH oxidation and acetylene addition surface reactions are modeled with elementary reaction Arrhenius equations by assuming chemical similarity [12]. That is, a surface reaction is similar to a reaction with a large PAH. The radical site fraction for surface reactions is based on the HACA model [15] and the active site fraction is based on the empirical model developed by Appel *et al.* [16] given by

$$\alpha = \tanh\left({a}/{\log(\mu)} + b\right) \tag{3}$$

where α is the active site fraction, μ is the first size moment, a and b are empirical parameters.

To use the stochastic soot simulations in a 3D domain, a Lagrangian-Eulerian framework is implemented. Each parcel passes its surrounding environment to an independent stochastic simulation as parameters. To couple the 0D soot simulations of the Lagrangian parcels to the Eulerian field, each parcel tracks the volume it represents and communicates with the Eulerian field in terms of densities. The volume representation is carefully tracked such that mass is conserved in exchanges between the two fields.

The Stokes number for particles smaller than 1000 nm is less than unity; accordingly, the motion of the parcels is assumed to perfectly follow the Eulerian gas phase. The thermal time constant of soot particles in standard combustion conditions is on the order of 100 nanoseconds or lower [17], which is more than an order of magnitude lower than the flow time scale. Accordingly, the parcel temperature is assumed to be at equilibrium with the surrounding gas. Lagrangian parcels are created as a function of the represented volume partition and local parcel divergence (i.e., $\nabla \cdot \rho_{parcel}$).

Like other soot model's, the stochastic soot model is solved in a time splitting fashion. Figure 1 is a flow chart of the soot model substep. The algorithm of Figure 1 runs the soot model until the surrounding environment of the parcel changes by `percentChange` to ensure stability and convergence. Then control returns to the gas phase chemistry solver. This coupling is limited by the slowest parcel in the domain.

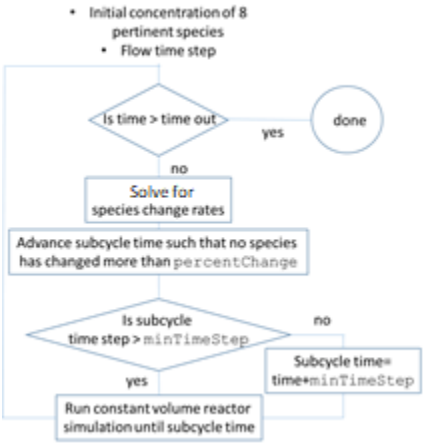

Figure 1 Simplified flow chart of chemistry/soot time step splitting algorithm

The hybrid model reduces the computational cost by removing the "weakest link" problem. Instead of using the stochastic model concurrently with the combustion model, it uses a standard fully coupled soot model as a surrogate to approximate the effect of soot as it would have been predicted by the directly coupled model.

Lagrangian parcels are still tracked and its surrounding conditions are logged. After the combustion simulation is complete, the parcel logs are fed into independent SWEEP simulations.

The hybrid model still requires access to the source code to produce the parcel logs, restricting its use in commercial codes. The hybrid model can be extended to these commercial codes by modifying the creation of Lagrangian parcels. The extended hybrid model uses a postprocessor to create parcels after the combustion simulation is completed. Parcels follow postprocessor calculated pathlines. The full and hybrid model parcels move according to the same equations. Parcels are initialized in isovolumes of a threshold inception species at regular times throughout the simulation such that all soot producing regions are adequately represented.

3. Hybrid Model Verification

The current CFD and chemical kinetics approach has been applied to a range of spray and engine combustion cases using a variety of fuels [18] [19]. For the sake of brevity, the present work will focus on validation of the hybrid and extended hybrid soot models.

Spray A experiments and case parameters [20] form the basis for Hybrid model verification because of its prevalence in literature, soot conducive conditions, and lack of additional confounding dynamic domain effects present in engine simulations. KIVA [21] and CONVERGE [22] CFD solvers were used. Both used the RANS framework.

The hybrid soot model relies on a conventional soot model to approximate the effects of soot as predicted by the more complex stochastic soot model that will follow. If the effects of temperature, species concentration, etc. are predicted poorly, the stochastic model will predict soot based on incorrect data. If, for example, the surrogate model predicts no changes, the results are the same as the stochastic model run in a one-way coupled mode. Figure 2 shows the predicted PSD for spray A at 1.75 ms after the start of injection for the two-way coupled, one-way coupled, and hybrid model. All simulations were performed in KIVA. The one-way coupled PSD reproduces the shape of the two-way coupled PSD, but over predicts the magnitude and maximum particle size. The overprediction is due to lack of consumption of pyrene in the one-way coupled approach. The hybrid model, using the method of moments as a surrogate, accurately captures both the shape and magnitude of the two-way coupled PSD to within one order of magnitude. Evidently, the surrogate model provides adequate likeness to the stochastic model to enable accurate soot prediction.

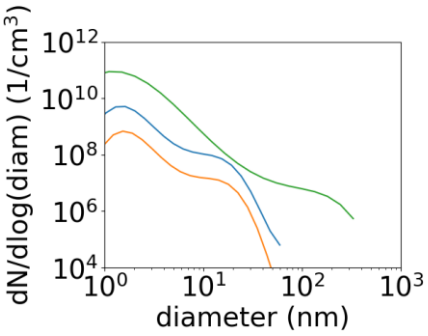

Figure 2 PSDs of Spray A at 1.75ms. Blue: Two-way coupled stochastic soot model, Green: one-way coupled model, and Orange: hybrid model with method of moments

The verification of the hybrid model showed that one-way coupling with a surrogate model is suitable for accurate soot prediction. While this is promising, it still requires substantial source code modification. To improve the usefulness of the code, a post-processing method was developed. We call this the extended hybrid model. The extended hybrid

soot model relies on post combustion simulation generated Lagrangian parcels to couple to the Eulerian field such that parcel representation is accurate. Figure 3 shows Spray A PSDs at multiple times using the standard hybrid model and the extended hybrid model with a method of moments surrogate soot model. Agreement is within an order of magnitude throughout. Discrepancies, such as, the inception mode particle population at 1ms are typically small and only temporary.

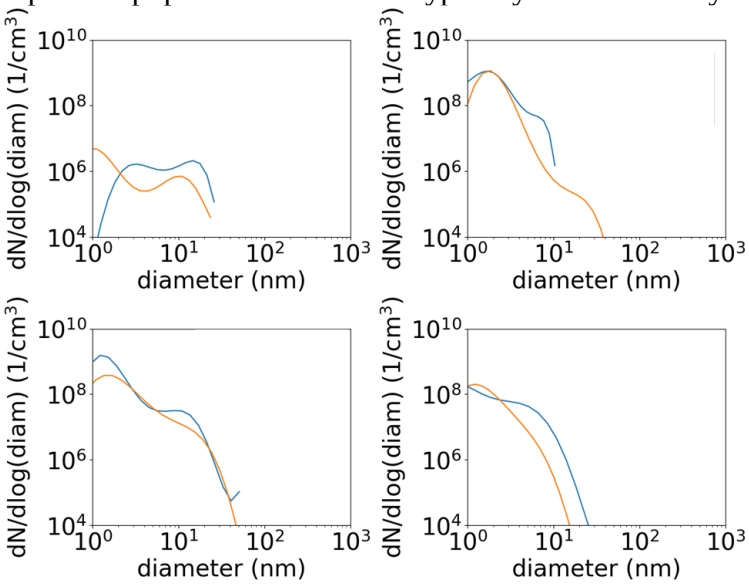

Figure 3 Top left: 1ms, Top right: 1.5ms, Bottom left: 2ms, Bottom right: 3.5ms. Blue: Extended hybrid model with Ensight generating and accumulating parcel histories, Orange: Conventional hybrid model with KIVA generating and tracking parcels.

4. Comparison with Existing Soot Models

The extended hybrid model was coupled with CONVERGE and comparisons were made between the extended hybrid model and commonly available soot models. The differences in PSDs between the SWEEP model and the sectional model are shown in Figure 4. The sectional model predicts a largely stagnant small mode particle population and the hybrid model predicts a dynamic growing population.

Figure 5 compares the Spray A PSDs produced using the extended hybrid model with multiple surrogate soot models. Although temporary similarities can be found, the accumulation mode for the sectional and method of moments models at 2ms for instance, there is not an easily identified standard PSD between the three surrogate models. The varying results summarized in Figure 5 highlights the importance of surrogate and stochastic model agreement.

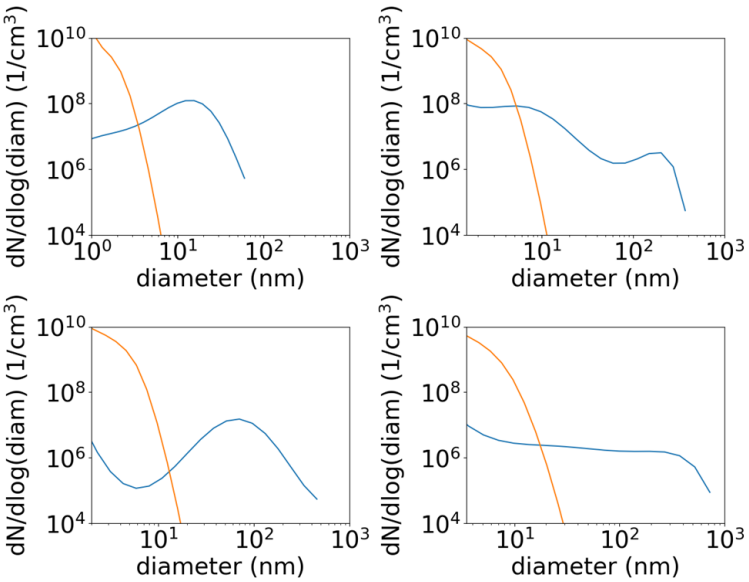

Figure 4 PSDs for the spray A conditions as predicted by indicated models at the indicated times. Top left: 1ms, Top right: 1.5ms, Bottom left: 2ms, Bottom right: 3.5ms. Blue: Extended hybrid model with a sectional surrogate soot model, Orange: Sectional soot model.

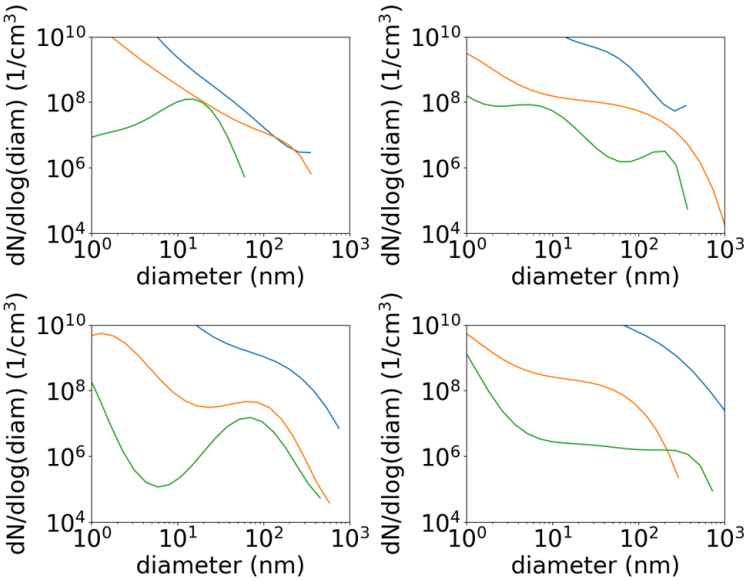

Figure 5 Top left: 1ms, Top right: 1.5ms, Bottom left: 2ms, Bottom right: 3.5ms. Blue: Hiroyasu, Orange: Method of moments model, Green: Sectional soot model. PSDs for the spray A conditions as predicted by indicated models at the indicated times.

5. Applying the Soot Model to a Diesel Engine

Simulations of a 1.9L GM diesel engine undergoing cold start cycles at 1500 rev/min and 2 bar IMEP with 3 injections were chosen based on the soot conducive conditions and the expected availability of detailed experimental data with particle size distributions to compare to. The third injection timing was swept from 9 to 21 deg. ATDC to provide a parameter effecting soot. CONVERGE and the extended hybrid model were used. The method of moments surrogate model was used because a similar method of moments surrogate model was used with KIVA in the validation step of Figure 3.

Figure 6 Shows PSD plots for the different third injection timings. Each plot shows PSDs at multiple crank angles. All cases have relatively similar soot populations at 10 deg ATDC because all of the cases are similar until the 3rd injection. Soot populations after the third injection vary greatly between the cases. When the third injection is later, the largest soot population is maximized at approximately 10 deg. ATDC. If the third injection is earlier, the largest particle population is maximized at approximately 50 deg. ATDC. The PSDs at EVO for the 9 and 13 deg. ATDC cases are very similar despite differences at earlier times. At 50 deg. ATDC the 13 deg. ATDC case has a much more pronounced bimodal distribution than the 9 deg ATD case.

Figure 7 (a) shows a scatter plot of the parcels, colored by soot mass fraction, at EVO. Soot mass is clearly concentrated in local pockets throughout the cylinder. Figure 7 (c) is filtered to only the 150 heaviest parcels and clarifies what was seen in Figure 7 (a). Namely, all of the high mass density soot regions are near a cylinder wall or piston face. The heaviest of the heavy are on

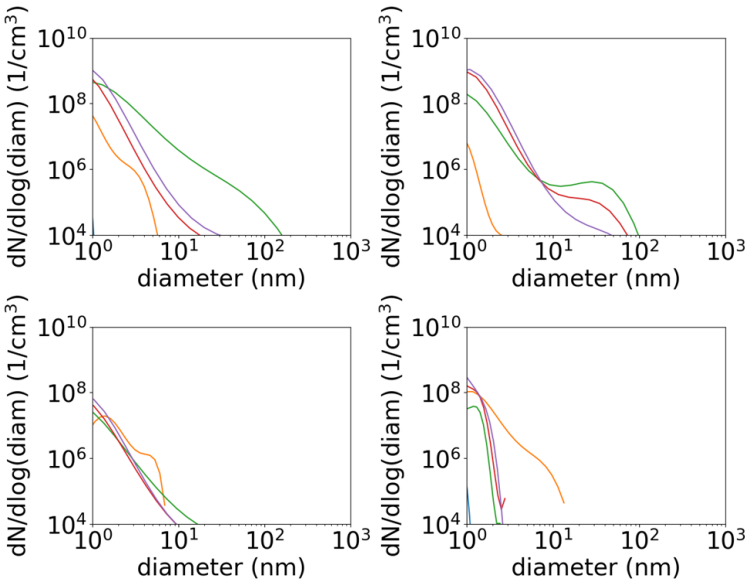

Figure 6 Top Left: Volume averaged PSDs for the diesel catalyst heating conditions. 9 deg. ATDC, Top Right: 13 deg. ATDC, Bottom Left: 17 deg. ATDC, Bottom Right 21 deg. ATDC, Orange: 10 deg. ATDC, Green: 50 deg. ATDC, Red: 85 deg. ATDC, Purple: 110 deg. ATDC.

the cylinder wall, halfway between the head and piston. Figure 7 (b) is a scatter plot with the same 150 parcels as Figure 7 (c) and colored the same way but located by where the soot parcel was born. Note that not all of the parcels were born at the same time. This plot shows that the heaviest parcels undergo a migration from the cylinder central volume to the cylinder walls. The heaviest parcels all start in a similar area, near the cylinder head and along the injection vector.

Figure 8 shows the particle size distribution at EVO for the entire volume and for only the boundary volume of the cylinder. This confirms that most of the soot is contained in the boundary volume at EVO. The final PSD on Figure 8 is also for the boundary volume but with parcels that started near the wall filtered out. This shows that most of the large particle population started away from the cylinder wall.

Figure 9 shows the path of the parcel with the highest contribution of soot mass to the cylinder volume at EVO. The parcel is created during the second injection far away from the cylinder wall. It is entrained in the 3rd injection and quickly brought to the cylinder wall. The parcel follows the cylinder wall until EVO.

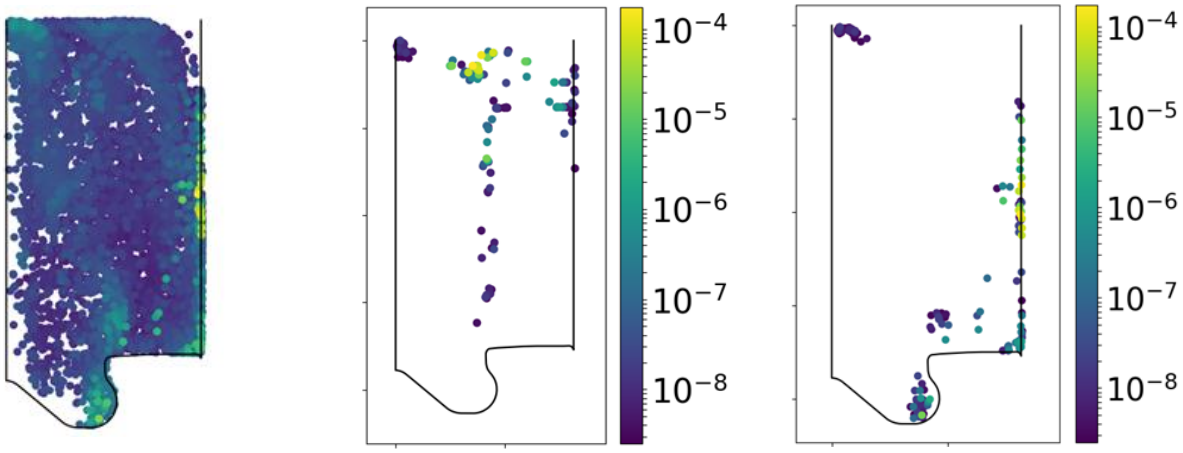

(a) (b) (c)

Figure 7 (a) Scatter plot of all soot parcels at EVO for 9 deg ATDC case. (b) Scatter plot of the location of generation of the 150 heaviest soot parcels at EVO for case with 3rd injection removed. Parcels are colored by mass fraction. (c) Scatter plot of 150 heaviest soot parcels at EVO for 9 deg. ATDC case. Parcels are colored by mass fraction

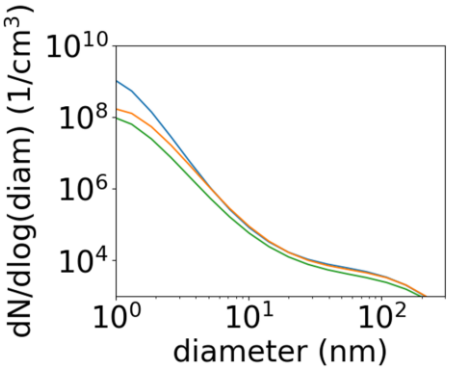

Figure 8 Blue: entire volume, Orange: volume near wall, Green: volume near wall with parcels that originated near wall filtered out. PSD of 9 deg. ATDC at EVO

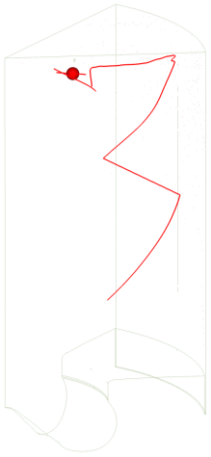

Figure 9 Path of heaviest parcel at EVO.

6. Conclusions

A hybrid variation of a stochastic soot model capable of running with limited computational resources and using conventional simulation software was introduced and validated in two stages. First, it was shown that using a surrogate soot model to consume inception species could produce accurate results. Second, it was shown that the Lagrangian soot parcels of the stochastic model could be created in a postprocessing step. The hybrid model was then used to show that a majority of the soot created in a diesel engine using a triple injection scheme originates near the center of the cylinder and moves to the perimeter in the entrainment of the third injection.

7. Acknowledgements

This material is based upon work supported by the Department of Energy, Office of Energy Efficiency and Renewable Energy (EERE) and the Department of Defense, Tank and Automotive Research, Development, and Engineering Center (TARDEC) under Award Number DE-EE0007300. The authors wish to thank Convergent Science Inc. for providing the licenses for the CONVERGE CFD solver.

8. References

[1] A. Fusco, A. L. Knox-Kelecy and D. E. Foster, "Application of a phenomenological soot model to diesel engine combustion," in *Proceedings of the International Symposium COMODIA*, 1994.

[2] F. Gelbard, Y. Tambour and J. H. Seinfeld, "Sectional representations for simulating aerosol dynamics," *Journal of Colloid and Interface Science*, vol. 76, pp. 541-556, 1980.

[3] M. Frenklach, "Computer modeling of infinite reaction sequences: A chemical lumping," *Chemical Engineering Science*, vol. 40, pp. 1843-1849, 1985.

[4] A. Kazakov and M. Frenklach, "Dynamic Modeling of Soot Particle Coagulation and Aggregation: Implementation With the Method of Moments and Application to High-Pressure Laminar Premixed Flames," *Combustion and Flame*, vol. 114, pp. 484-501, 1998.

[5] M. Celnik, A. Raj, R. West, R. Patterson and M. Kraft, "Aromatic site description of soot particles," *Combustion and Flame,* vol. 155, pp. 161-180, 2008.

[6] N. Morgan, M. Kraft, M. Balthasar, D. Wong, M. Frenklach and P. Mitchell, "Numerical simulations of soot aggregation in premixed laminar flames," *Proceedings of the Combustion Institute,* vol. 31, pp. 693-700, 2007.

[7] M. Balthasar and M. Kraft, "A stochastic approach to calculate the particle size distribution function of soot particles in laminar premixed flames," *Combustion and Flame,* vol. 133, pp. 289-298, 2003.

[8] T. Strickland and S. Kokjonh, "Simulation of a diesel fuel jet with a 3D stochastic soot model," in *2018 Spring Technical Meeting Central States Section of The Combustion Institute,* Minneapolis, 2018.

[9] R. I. A. Patterson, J. Singh, M. Balthasar, M. Kraft and J. R. Norris, "The Linear Process Deferment Algorithm: A new technique for solving population balance equations," *SIAM Journal on Scientific Computing,* vol. 28, pp. 303-320, 2006.

[10] M. Celnik, R. Patterson, M. Kraft and W. Wagner, "Coupling a stochastic soot population balance to gas-phase chemistry using operator splitting," *Combustion and Flame,* vol. 148, pp. 158-176, 2007.

[11] M. Goodson and M. Kraft, "An Efficient Stochastic Algorithm for Simulating Nano-particle Dynamics," *Journal of Computational Physics,* vol. 183, pp. 210-232, 2002.

[12] M. Frenklach, "Reaction mechanism of soot formation in flames," *Physical chemistry chemical Physics,* vol. 4, pp. 2028-2037, 2002.

[13] R. I. A. Patterson, J. Singh, M. Balthasar, M. Kraft and W. Wagner, "Extending stochastic soot simulation to higher pressures," *Combustion and Flame,* vol. 145, pp. 638-642, 2006.

[14] H. F. Calcote and D. M. Manos, "Effect of molecular structure on incipient soot formation," *Combustion and Flame,* vol. 49, pp. 289-304, 1983.

[15] M. Frenklach and H. Wang, "Detailed mechanism and modeling of soot particle formation," in *Soot formation in combustion,* Springer, 1994, pp. 165-192.

[16] J. Appel, H. Bockhorn and M. Frenklach, "Kinetic modeling of soot formation with detailed chemistry and physics: laminar premixed flames of C2 hydrocarbons," *Combustion and flame,* vol. 121, pp. 122-136, 2000.

[17] F. Liu, K. J. Daun, D. R. Snelling and G. J. Smallwood, "Heat conduction from a spherical nano-particle: status of modeling heat conduction in laser-induced incandescence," *Applied physics B,* vol. 83, pp. 355-382, 2006.

[18] F. D. F. Chuahy and S. L. Kokjohn, "High efficiency dual-fuel combustion through thermochemical recovery and diesel reforming," *Applied Energy,* vol. 195, pp. 503-522, 2017.

[19] C. Kavuri, J. Paz and S. L. Kokjohn, "A comparison of Reactivity Controlled Compression Ignition (RCCI) and Gasoline Compression Ignition (GCI) strategies at high load, low speed conditions," *Energy Conversion and Management,* vol. 127, pp. 324-341, 2016.

[20] L. M. Pickett, C. L. Genzale, G. Bruneaux, L.-M. Malbec, L. Hermant, C. Christiansen and J. Schramm, "Comparison of Diesel Spray Combustion in Different High-Temperature, High-Pressure Facilities," *SAE International Journal of Engines,* vol. 3, no. 2, pp. 156-181, 2010.

[21] A. A. Amsden and M. Findley, "KIVA-3V: A block-structured KIVA program for engines with vertical or canted valves," 1997.

[22] K. J. Richards, P. K. Senecal and E. C. O. N. V. E. R. G. E. Pomraning, "CONVERGE 2.1. 0 Theory Manual, Convergent Science," *Inc., Middleton, WI,* 2013.